International Journal of Academic Research
ISSN: 2360-9909.Volume 13, Issue 3, (August, 2022) pages 40 - 54
DOI:2726145271334
www.arcnjournals.org

Kinetics of Thiosulphate ion Oxidation by Methyl Green in Acidic Medium

Aishatu M. Bulama[1], Bahijja G. Ahmad[2] and Aisha M. Ngubdo[3]
[1&3]Department of Remedial Sciences, Ramat Polytechnic Maiduguri, Borno State, Nigeria.
[2]Department of Chemistry, University of Maiduguri, Borno State, Nigeria.
Corresponding author: aishamusabulama91@gmail.com

Abstract: *The kinetics of the thiosulphate ($S_2O_3^{-2}$) oxidation of methyl green (MG^{2+}) have been studied in aqueous acidic medium. The observed results at $[H^+] = 1.0 \times 10^{-4}$ mol dm^{-3}(HCl), ionic strength of the reaction medium, $\mu = 0.06$ mol dm^{-3} (NaCl) and $T = 29.0 \pm 1^oC$ are consistent with the rate law: $d[MG^{2+}]/dt = k_2[MG^+][S_2O_3^{2-}]$. The reaction was found to be first order with respect to MG^{2+} and was catalyzed by increase in μ and added anions. Increase in $[H^+]$, cations and dielectric constant inhibited the reaction. Spectrophotometric test showed the absence of intermediate complex formation. Based on these findings, a plausible mechanism is proposed.*

Key words: *kinetics, thiosulphate, methyl green, acidic medium, spectroscopic test, mechanism*

INTRODUCTION

Methyl Green (MG^{2+}) is a basic triphenylmethane-type dicationic dye with IUPAC name [4-[(4-dimethyl aminophenyl) -4- dimethylazaniumylidene cyclohexa -2, 5-diene-1-ylidene) methyly)phenyl]–trimethly-azanium dichloride). Methyl green is usually used for staining solution in medicine and biology and as a photochromophore to sensitize gelatinous films (Mai *et al.,* 2008). Cationic (basic) dyes have been used for paper, polyacrylonitrile, modified polyesters, polyethylene terephthalate and to some extent, in medicine. Originally they were used for silk, wool and tannin-mordanted cotton. These water soluble dyes yield coloured cations, in solution and that is why they are called cationic dyes (Gupta and Suhas, 2009).

Sodium thiosulphate ($Na_2S_2O_3$), is an inorganic compound that is typically available as the penta hydrate ($Na_2S_2O_3.5H_2O$). The solid is an efflorescent (loses water readily) crystalline substance that dissolves well in water. It is also called sodium hyposulphite or 'hypo' (Barbera *et al.,* 2012). Sodium thiosulphate has found a variety of applications in different fields. It is used for both film and photographic paper processing, the sodium thiosulphate is known as a photographic fixer, and is often referred to as 'hypo' from the original name, hyposulphate of soda (Gibson, 1908). Sodium thiosulphate is also used to dechlorinate tap water including lowering chlorine levels for use in aquaria and swimming pools and spas (e.g following superchlorination) and within water treatment plants to treat settled backwash water prior to release into rivers (Barbera *et al.,* 2012). In medicine, it has been used as treatment of calciphylaxis in hemodialysis patients with end stage kidney disease (Cicone *et al.,* 2004). There is apparently an incompletely understood phenomenon whereby this causes severe metabolic

acidosis in some patients (Selk and Rodby, 2010). It is used as an antidote to cyanide poisoning. (Hall *et al*., 2007).

However, kinetic data on the decolourization of MG^{2+} is scanty in literature, this bring the interest to study kinetics of thiosulphate ion oxidation by methyl green under acidic medium.

2.0 EXPERIMENTAL

2.1 Materials

All chemical reagents used were of analytical grade (BDH, Kernel, Sigma-Aldrich) and were used without further purification. Distilled water was used throughout for all solution preparation.

2.2 Methods

2.2.1 Stoichiometric studies

Spectrophotometric titration was obtained using the mole ratio method to determine the stoichiometry of the reaction, at $[MG^{+2}] = 4.8 \times 10^{-5}$ mol dm^{-3}, $[S_2O_3^{-2}] = (0.48 – 4.8) \times 10^{-4}$ mol dm^{-3}, $[H^+] = 1.0 \times 10^{-4}$ mol dm^{-3}, $\mu = 0.06$ mol dm^{-3}(NaCl). The absorbance of the reaction mixture at 630 nm were measured until the completion of the reaction was indicated by a constant absorbance value. Plots of absorbance (A_∞) versus mole ratio revealed the stoichiometry of the reaction.

2.2.2 Kinetic Measurement

The rate of reaction was studied by monitoring the decrease in the absorbance of methyl green at 630 nm, using 721 visible spectrophotometer after it has been established that none of the reactants have any significant absorbance at this wavelength.

All the kinetic measurements were carried out under pseudo–first order conditions with the concentration of $S_2O_3^{2-}$ at least 1000-fold excess over that of the methyl green at temperature of 29.0 ± 1.0ºC, ionic strength of 0.06 mol dm^{-3}(NaCl) and $[H^+] = 1.0 \times 10^{-4}$ mol dm^{-3}(HCl).

The pseudo – first order plots of log ($A_t – A_\infty$) against time were made and the slope of the plots gave the pseudo – first order rate constants, k_1 (Osunlaja, 2013). The second order rate constants, k_2, were determined from k_1 as $k_1/ [S_2O_3^{2-}]$.

The effect of changes in $[H^+]$ on the reaction rate was investigated by keeping $[MG^{2+}]$ and $[S_2O_3^{2-}]$ constant while varying $[H^+]$ between 2.0 x 10^{-5} and 2.0 x 10^{-4} mol dm^{-3}, ionic strength, μ, was maintained at 0.06 mol dm^{-3} (NaCl) and reaction was carried out at 29.0 ± 1.0°C.

Order of reaction with respect to $[H^+]$ was obtained as the slope of the plot of log k_1 against log $[H^+]$. Variation of acid dependent second order rate constant with $[H^+]$ was obtained by plotting k_{H+} against $[H^+]$.

The ionic strength of the reaction mixture was varied between 0.02 and 0.20 mol dm^{-3} and maintaining [MG^{2+}], [$S_2O_3^{2-}$] and [H^+] constant. Reaction temperature was maintained at 29.0 ± 1.0°C. Relationship of reaction rate with changes in the ionic strength was determined by plotting log k_2 against μ.

Binary solvent mixture of water and acetone were used to investigate the effect of change in dielectric medium on the rates of reaction at the dielectric constant of 80.4 – 66.0 (1 – 5)% acetone. All the reactants were kept constant except for the binary mixtures which were varied in the percentage of 1 – 5. As the dielectric constants decreases from 80.4 – 66.0, keeping [MG^{2+}], [$S_2O_3^{2-}$] and [H+] constant. The ionic strength of 0.06 mol dm^{-3} and temperature of 29.0 ± 1.0°C were maintained. A plot of log k_2 against 1/D gives the relationship between the second order rate constant and the total dielectric constant of the reaction medium, D.

The effect of added cations on the reaction rate was investigated by the addition of 2.0 x 10^{-2} to 1.0 x 10^{-1} mol dm^{-3} of (Li^+ and K^+) keeping [MG^{2+}], [$S_2O_3^{2-}$] and [H^+] constant. The ionic strength of 0.06 mol dm^{-3} and temperature of 29.0 ± 1.0°C were maintained.

The effect of added anion on the reaction rate was observed by introducing 2.0 × 10^{-4} to 1.0 × 10^{-3} of (NO_3^-) keeping all the reactants constant, temperature was also maintained.

The reaction mixture was tested for possible free radicals by adding acrylamide to the mixture followed by excess methanol. Any polymerization evidenced by gel formation would provide a suspicion for the presence of free radicals in the reaction mixture.

3.0 Results and Discussions

3.1 Stoichiometry

Stoichiometry results for the reduction of MG^{2+} by $S_2O_3^{-2}$ revealed that one mole of MG^{2+} was reduced by three moles of $S_2O_3^{2-}$ which is consistent with the equation 1, and the plot of absorbance against mole ratio is represented in Figure 1.

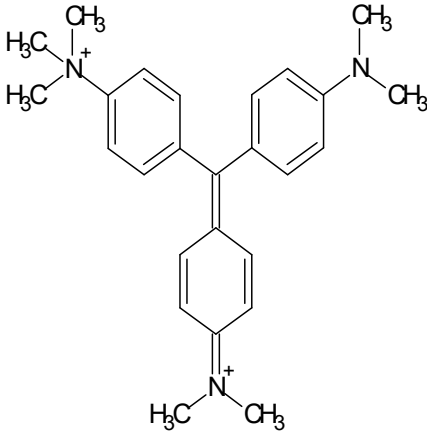

Methyl Green

$$+ 4S_2O_3^{2-} + H_2O \rightarrow LMG + 2S_4O_6^{2-} + H^+ \ldots 1$$

where LMG = Leucomethyl greeen

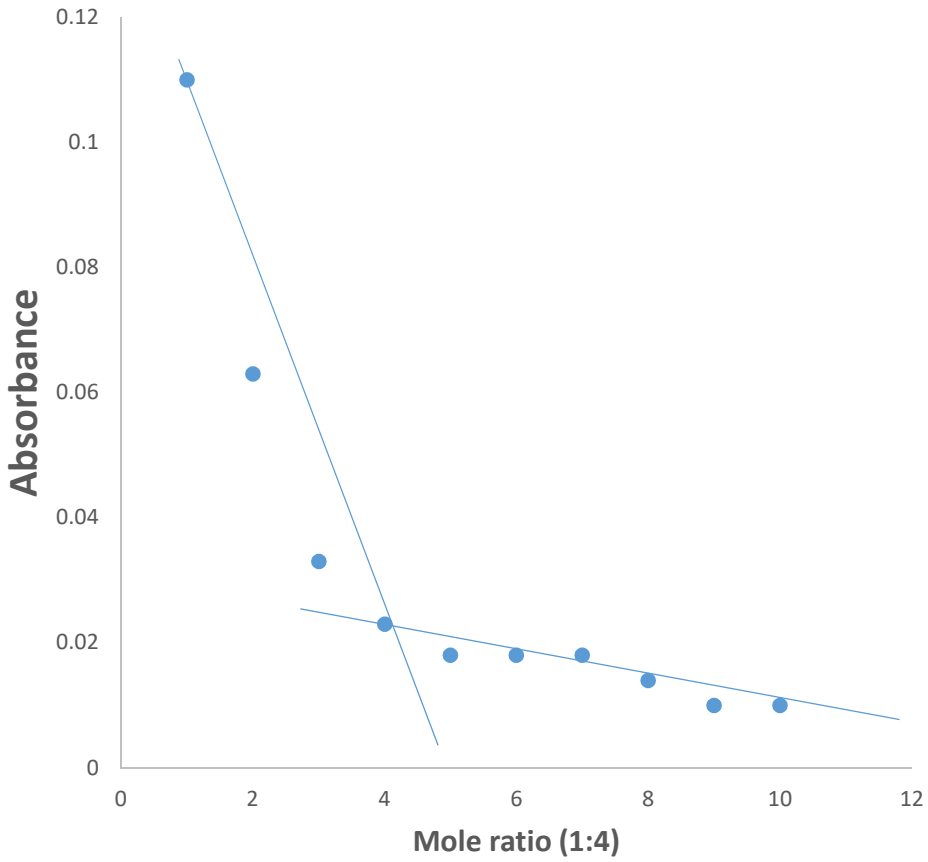

Figure 1: Plot of absorbance versus mole ratio for the determination of stoichiometry of the reduction of MG^{+} by $S_2O_3^{-2}$ at $[MG^{+}] = 4.8 \times 10^{-5}$ mol dm^{-3}, $[S_2O_3^{-2}] = (0.48 - 4.8) \times 10^{-4}$ mol dm^{-3}, $[H^{+}] = 1.0 \times 10^{-4}$ mol dm^{-3}, $\mu = 0.06$ mol dm^{-3}(NaCl), T = 29.0 ± 1.0^{o}C and λ_{max} = 630 nm

3.2 Order of the Reaction

Pseudo first order plots of log (A_t - A_∞) versus time were linear to about 70 – 80% in the reaction. This indicate that the reaction is first order with respect to $[MG^{2+}]$. The typical pseudo – first order plot is shown in Figure 2. Linear plots of log k against log $[S_2O_3^{2-}]$ with a slope of 1.03 confirmed the reaction to be first order with respect to $[S_2O_3^{2-}]$ which is presented in Figure 3. The reaction is second order overall and the rate constants obtained from the equation $k_2 = k_1/[S_2O_3^{2-}]$ were found to be fairly constant (Table 1) and the average was found to be $(4.8 \times 10^{-2}) \pm 0.005$ dm^3 mol^{-1} s^{-1}

The rate equation can be presented as:

$$dMG^{2+}/dt = k_2[MG^{2+}][S_2O_3^{2-}] \quad \ldots\ldots 2$$

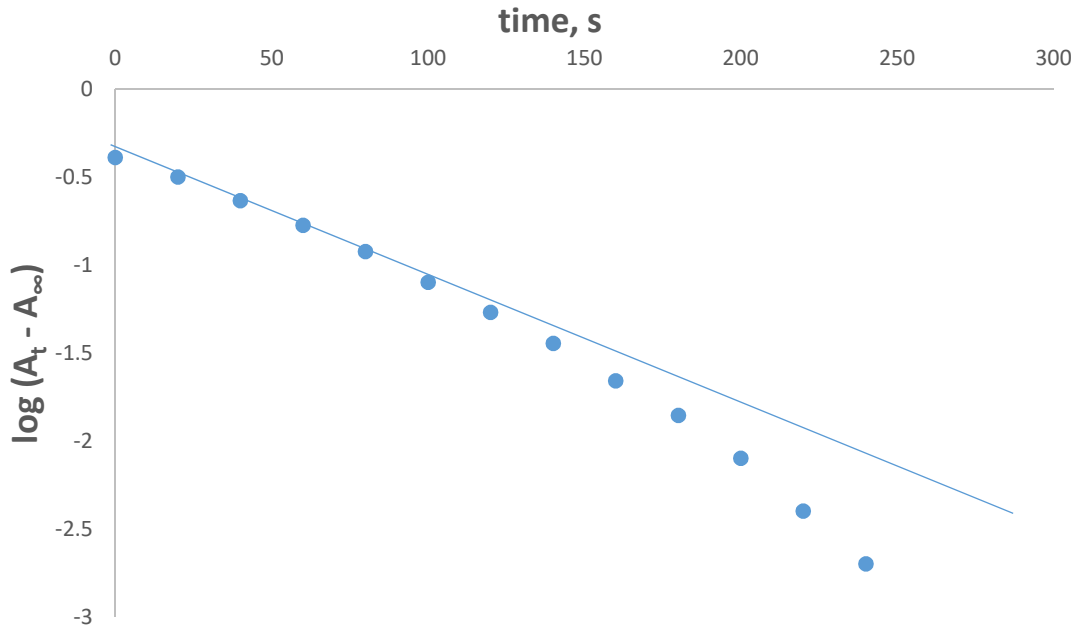

Figure 2: Pseudo-first order plot for the oxidation of $S_2O_3^{-2}$ by MG^+ at $[MG^+] = 4.8 \times 10^{-5}$ mol dm^{-3} $[S_2O_3^{-2}]$ 0.480 mol dm^{-3}, $[H^+] = 1.0 \times 10^{-4}$, $\mu = 0.06$ mol dm^{-3} NaCl), T = 29.0 ± 1°C and $\lambda_{max} = 630$ nm

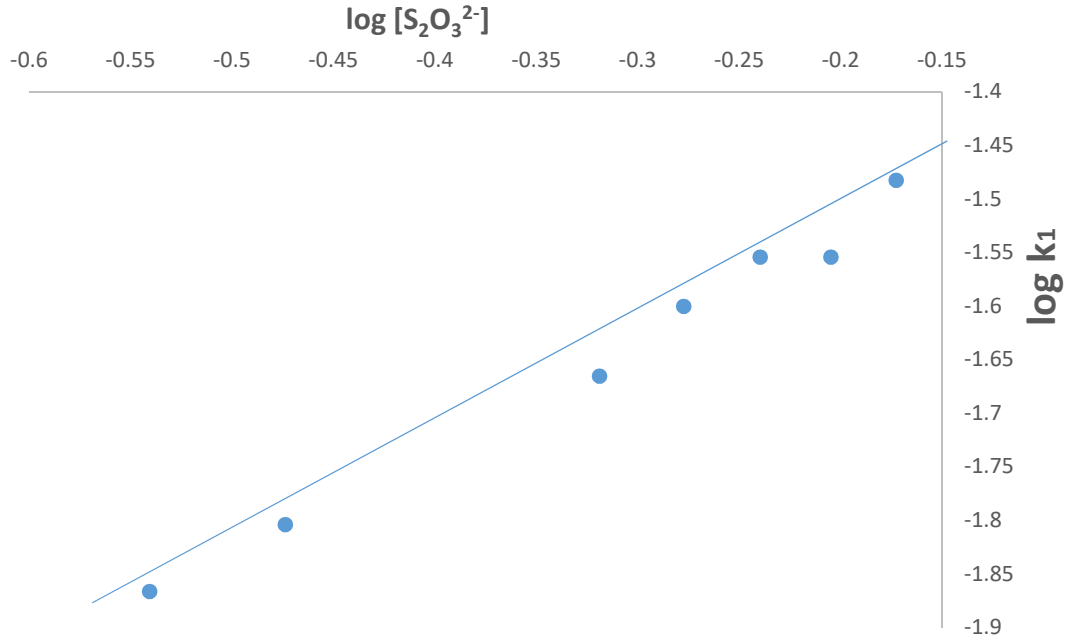

Figure 3: Plot of log k_1 against log $[S_2O_3^{-2}]$ for the oxidation of $S_2O_3^{-2}$ by MG^{2+} at $[MG^{2+}] = 4.8 \times 10^{-5}$ mol dm^{-3}, $[S_2O_3^{-2}]$ = (0.288 – 0.672) mold m^{-3}, $[H^+] = 1.0 \times 10^{-4}$mol dm^{-3}, μ = 0.06mol dm^{-3} (NaCl), T = 29.0 ± 1.0°C and $\lambda_{max} = 630$ nm

Table 1: Pseudo-first order rate constants for the reaction of MG^{2+} with $S_2O_3^{2-}$ at $[MG^{2+}] = 4.8 \times 10^{-5}$ mol dm^{-3}, $\lambda_{max} = 630$ nm and T = 29.0 ± 1.0°C

$10^2[S_2O_3^{2-}]$ (mol dm^{-3})	$10^5[H^+]$ (mol dm^{-3})	$10^3\mu$ (mol dm^{-3})	10^3k_1 (s^{-1})	10^2k_2 (dm^3 mol^{-1} s^{-1})
2.88	10.0	60	13.6	4.7
3.36	10.0	60	15.7	4.7
4.80	10.0	60	23.0	4.8
5.28	10.0	60	25.1	4.8
5.76	10.0	60	27.9	4.8
6.24	10.0	60	27.9	4.5
6.72	10.0	60	32.9	4.9
4.80	2.0	60	39.8	8.3
4.80	4.0	60	32.7	6.8
4.80	6.0	60	32.2	6.7
4.80	8.0	60	24.2	5.0
4.80	10.0	60	23.0	4.8
4.80	12.0	60	21.9	4.6
4.80	14.0	60	20.5	4.3
4.80	16.0	60	19.6	4.1
4.80	18.0	60	19.1	4.0
4.80	20.0	60	18.2	3.8
4.80	10.0	20	19.6	4.1
4.80	10.0	40	20.7	4.3
4.80	10.0	60	23.0	4.8
4.80	10.0	80	26.3	5.4
4.80	10.0	100	26.5	5.5

4.80	10.0	120	27.8	5.8
4.80	10.0	140	27.8	5.8
4.80	10.0	160	28.8	5.9
4.80	10.0	180	29.0	6.0

3.3 Effect of change in Hydrogen ion concentration

The effect of changes in $[H^+]$ on the rates of reaction was determined by varying the concentrations of HCl at $(0.2 – 2.0) \times 10^{-4}$ mol dm^{-3}. The acid dependent rate constants obtained showed that the rate of reaction decreased with increase in $[H^+]$ (Table 1). Plot of k_{H+} versus $1/[H^+]$ showed the dependence of the second order rate constants on $[H^+]$ for the reaction (Figure 4) and the plot is linear with a positive intercept. Plot of log k_1 versus log $[H^+]$ was linear indicating first order with respect to $[H^+]$ (Figure 5). The H^+ dependent second order rate constant can thus be presented by equation 3:

$$k_{H+} = a + b[H^+]^{-1} \quad \ldots\ldots 3$$

'a' = 4.8×10^{-2} dm^3 mol^{-1} s^{-1} and 'b' = 1.8 dm^6 mol^{-2} s^{-1}.

In the range of $[H^+]$ used, the overall rate equation can be represented by equation 4 below:

$$-d[MG^{2+}]/dt = (a + b[H^+]^{-1})[MG^{2+}][S_2O_3^{2-}] \quad \ldots\ldots 4$$

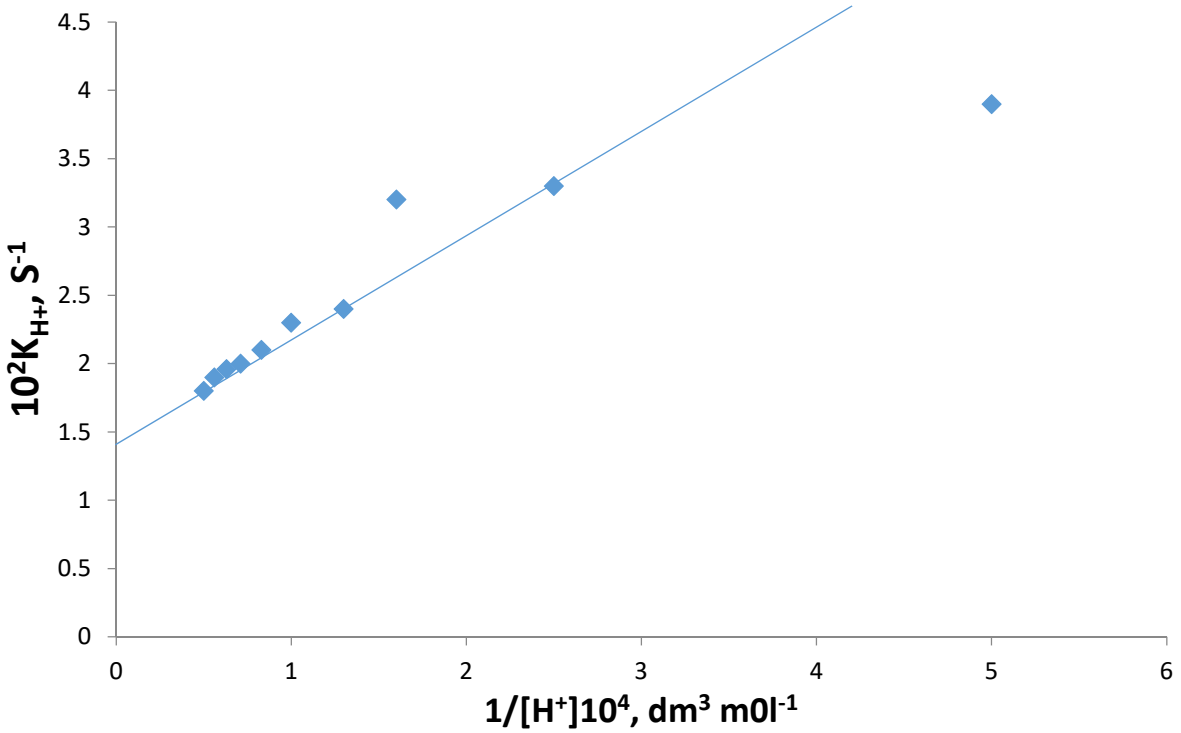

Figure 4: Plot of k_{H+} versus $1/[H^+]$ for the reaction of MG^{2+} with $S_2O_3^{-2}$ at $[MG^{2+}] = 4.8 \times 10^{-5}$ mol dm^{-3}, $[S_2O_3^{-2}] = 0.48$ mol dm^{-3}, $[H^+] = (0.8 – 2.0) \times 10^{-4}$ mol dm^{-3}, $\mu = 0.06$ mol dm^{-3} (NaCl), T = 29.0 ±1.0°C and $\lambda_{max} = 630$ nm

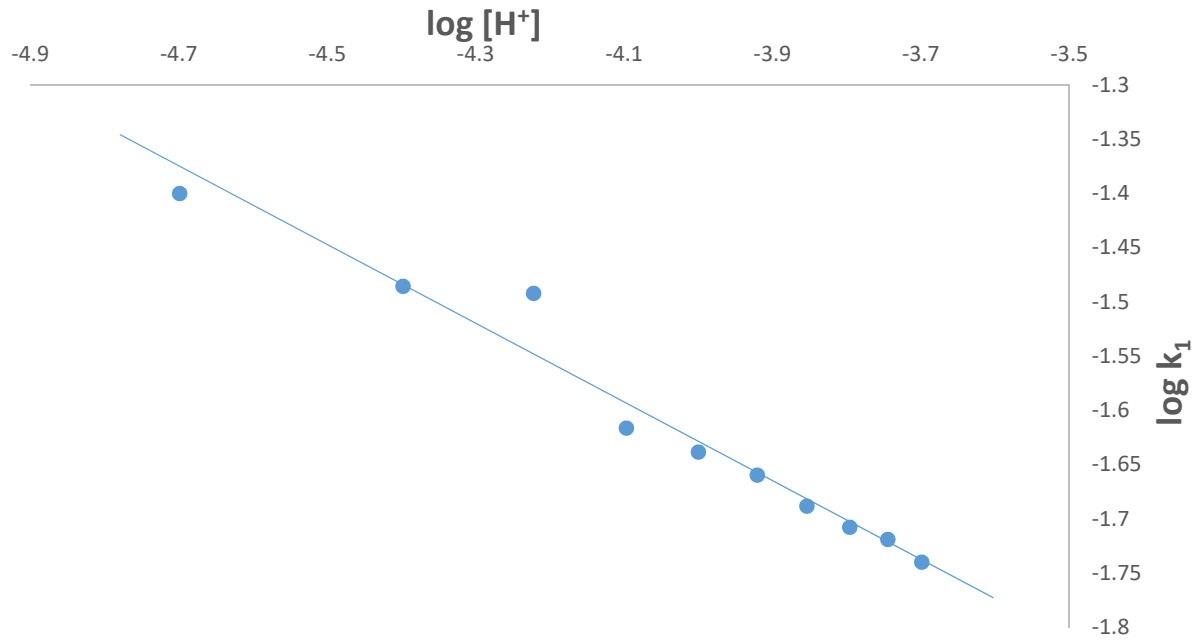

Figure 5: Plot of log k_1 against log $[H^+]$ for the reaction between MG^{2+} and $S_2O_3^{2-}$ at $[MG^{2+}] = 4.8 \times 10^{-5}$ mol dm^{-3}, $[S_2O_3^{-2}] = 4.8 \times 10^{-1}$ mol dm^{-3}, $[H^+] = (0.2 – 2.0) \times 10^{-4}$ mol dm^{-3}, $\mu = 0.06$ mol dm^{-3} (NaCl), T = 29.0 ± 1.0°C and $\lambda_{max} = 630$ nm.

3.4 Effect of change in ionic strength concentration and added anions

The rates of the reaction were found to increase with increase in the ionic strength (Table 1) and added anions (Table 2). This catalytic effect shown by the addition of anions is possibly due to coulombic bridging in which the closeness of approach of the reactant ions in the activated complex is such as to allow added ions to come in between them, thereby affecting the rates of reaction. This is seen when the reaction is proceeding through the outer sphere pathway in which the reactant ions maintain their coordination integrity in the activated complex prior to and during electron transfer(Mohammed et al.,2009) Plot of log k_2 versus $\sqrt{\mu}$ showed the relationship of reaction rates with changes in the ionic strength which is represented in Figure 6 and the least square plot of dependence of k_2 on [X] for added anion is represented in Figure 7.

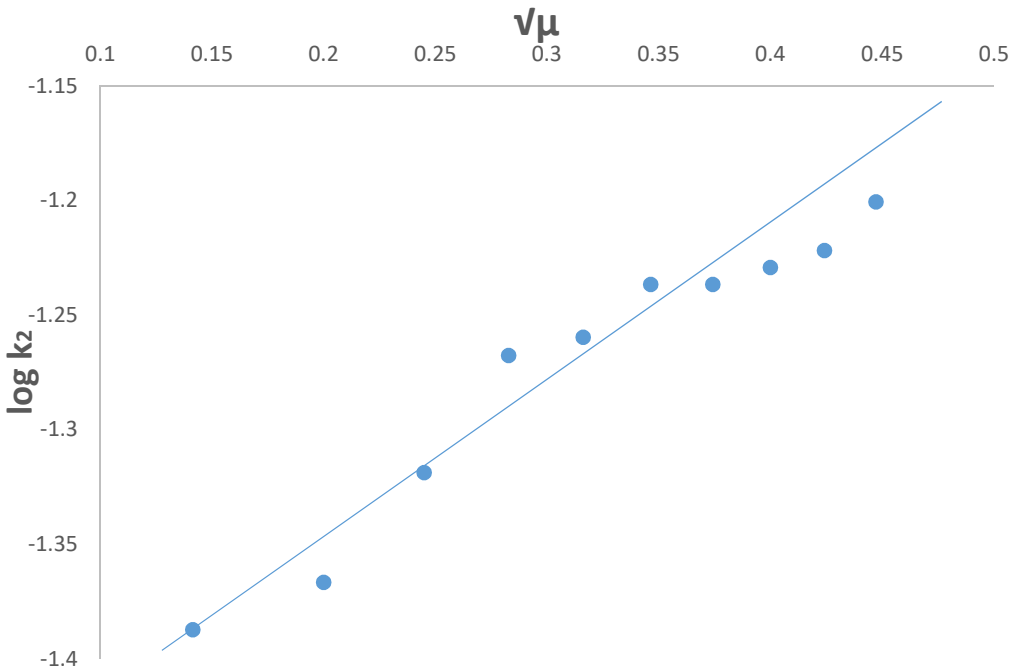

Figure 6: Plot of log k_2 against √μ for the reduction of MG^{2+} by $S_2O_3^{-2}$ at $[MG^{2+}] = 4.8 \times 10^{-5}$mol dm^{-3}, $[S_2O_3^{-2}] = .480$ mol dm^{-3}, $[H^+] = 1.0 \times 10^{-4}$ mol dm^{-3}, μ = 0.02 – 0.20 mol dm^{-3} (NaCl), T = 29.0 ± 1.0°C and λ_{max} = 630 nm

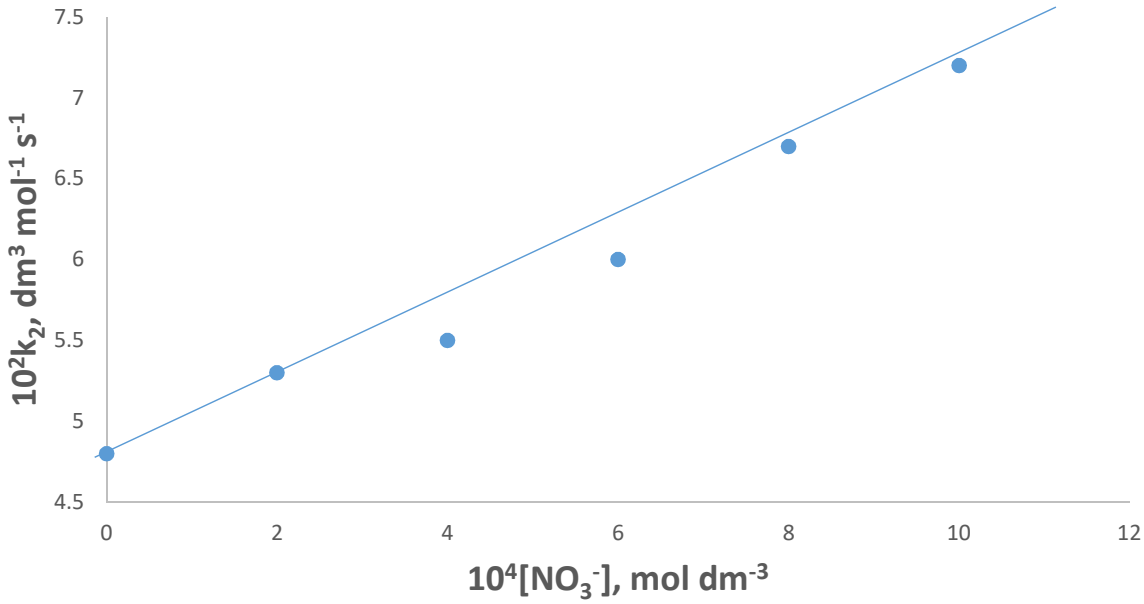

Figure 7: Plot of dependence of k_2 on $[NO_3^-]$ for the reaction of MG^{2+} with $S_2O_3^{2-}$ at $[MG^{2+}] = 4.8 \times 10^{-5}$ mol dm^{-3}, $[S_2O_3^{2-}] = 0.480$ mol dm^{-3}, $[H^+] = 1.0 \times 10^{-4}$ mol dm^{-3}, μ = 0.06 mol dm^{-3}(NaCl), λ_{max} = 630 nm and T = 29.0 ± 1.0°C

Table 2: Rate data for the effect of cations and anions on the second order rate constant for MG^{2+} and $S_2O_3^{2-}$ reaction at $[MG^{2+}] = 4.8 \times 10^{-5}$ mol dm^{-3}, $[S_2O_3^{2-}] = 0.480$ mol dm^{-3}, $[H^+] = 1.0 \times 10^{-4}$ mol dm^{-3}, $\mu = 0.06$ mol dm^{-3} (NaCl), $\lambda_{max} = 630$ nm and $T = 29.0 \pm 1.0^oC$

X	10^4[X] mol dm^{-3}	10^2k_1 (s^{-1})	10^2k_2 (dm^3 $mol^{-1}s^{-1}$)
Li^+	0	2.30	4.80
	200	1.98	4.10
	400	1.41	2.90
	600	1.31	2.70
	800	1.11	2.30
	1000	0.89	1.90
K^+	0	2.30	4.80
	200	1.70	3.60
	400	1.45	3.00
	600	1.34	2.80
	800	1.11	2.30
	1000	0.89	1.90
NO_3^-	0	2.30	4.80
	2.0	2.56	5.30
	4.0	2.63	5.50
	6.0	2.90	6.00
	8.0	3.20	6.7
	10.0	3.48	7.2

3.5 Effect of change in Dielectric constant and added cations

The rates of the reaction were found to decrease with increase in the percentage of acetone (Table 3) and added cations (Table 2). Plot of log k_2 versus 1/D showed the dependence of the second order rate constants on the dielectric constant of the reaction medium (Figure 8) and the

plot of dependence of k_2 on [Y] which is represented in Figure 9 showed the dependence of k_2 on the concentration of the added cation.

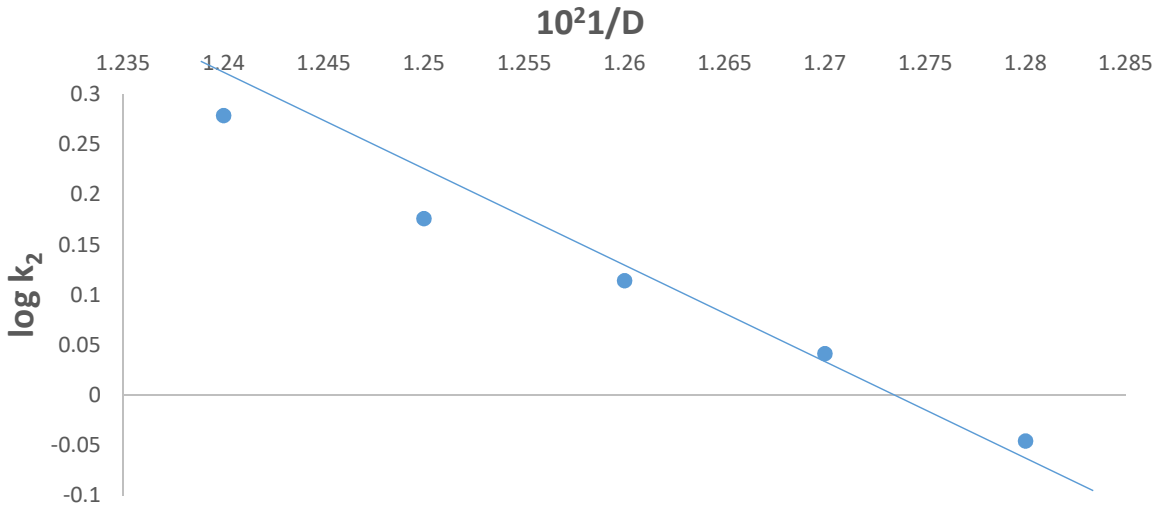

Figure 8: Plot of log k_2 against 1/D for the reduction of MG^{2+} by $S_2O_3^{2-}$ at $[MG^{2+}] = 4.8 \times 10^{-5}$ mol dm^{-3}, $[S_2O_3^{2-}] = 0.480$ mol dm^{-3}, $[H^+] = 1.0 \times 10^{-4}$ mol dm^{-3}, $\mu = 0.06$ mol dm^{-3}(NaCl), T = 29.0 ± 1.0°C and $\lambda_{max} = 630$ nm

Table 3: Effect of changes in the dielectric constant for the oxidation of $S_2O_3^{2-}$ by MG^{2+} at $[MG^{2+}] = 4.8 \times 10^{-5}$ mol dm^{-3}, $[S_2O_3^{2-}] = 0.480$ mol dm^{-3}, $[H^+] = 1.0 \times 10^{-4}$ mol dm^{-3}, $\mu = 0.06$ mol dm^{-3}(NaCl), T = 29.0 ± 1.0°C and $\lambda_{max} = 630$ nm

D	10^2 1/D	$10^3k_1(s^{-1})$	10^2k_2 (dm^3 mol^{-1} s^{-1})
80.4	1.24	9.21	1.9
79.8	1.25	7.37	1.5
79.2	1.26	6.45	1.3
78.6	1.27	5.29	1.1
78.0	1.28	4.15	0.9

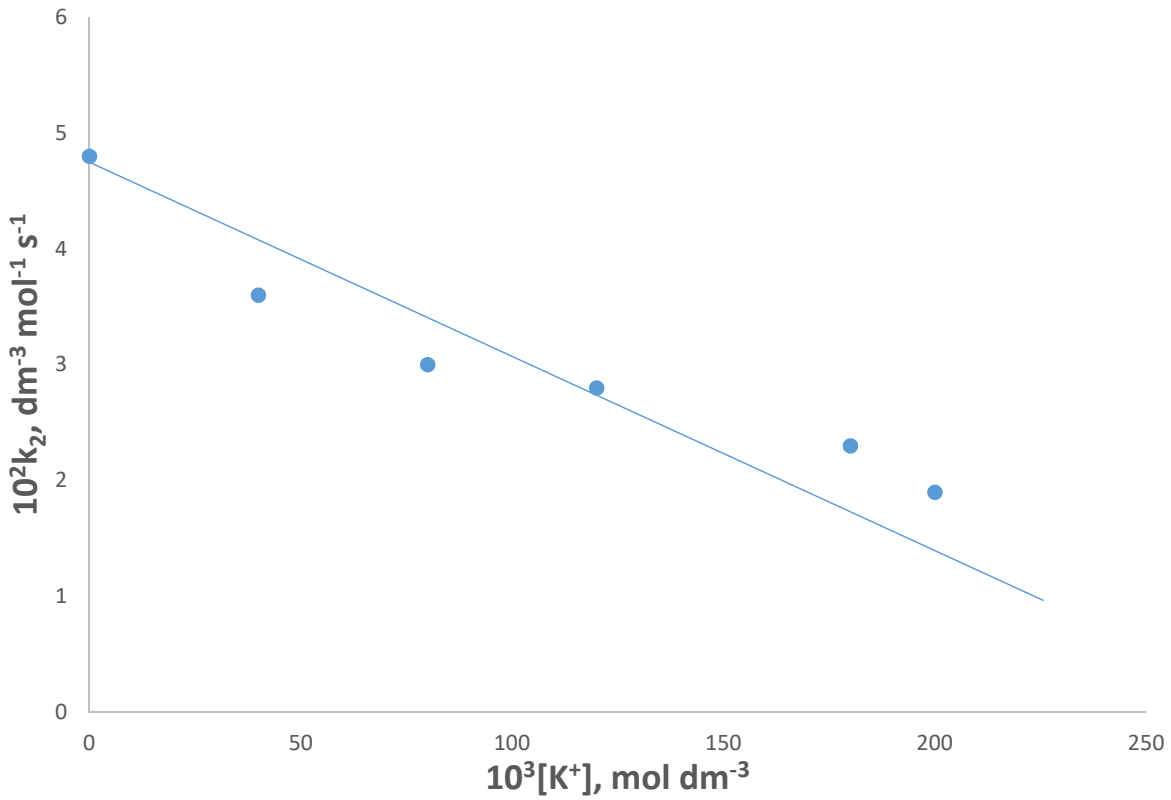

Figure 9: Plot of dependence of k_2 on $[K^+]$ for the reaction of MG^{2+} with $S_2O_3^{2-}$ at $[MG^{2+}] = 4.8 \times 10^{-5}$ mol dm^{-3}, $[S_2O_3^{2-}] = 0.480$ mol dm^{-3}, $[H^+] = 1.0 \times 10^{-4}$ mol dm^{-3}, $\mu = 0.06$ mol dm^{-3}(NaCl), $\lambda_{max} = 630$ nm and $T = 28.0 \pm 1.0^oC$

3.6 Product Analysis

After the completion of the reaction, a colourless solution was obtained and the UV visible spectra of the product showed no absorption peak at λmax of 630 nm. This indicates the destruction of the quinoid (chromophore) group. Furthermore, on addition of mercury (I) nitrate to the reaction solution produced a yellow precipitate, which became black on heating, thus indicating the presence of tetrathionate ions ($S_4O_6^{2-}$).

3.7 Free Radicals

Addition of a solution of acrylamide to partially reacted mixture did not give a gel in the presence of excess methanol, indicating the probable absence of free radicals in the reaction mechanism.

3.8 Spectroscopic Test for Intermediate Complex Formation

The plot of $1/k_1$ vs $1/ [S_2O_3^{2-}]$ gave a straight line which passed through the origin (Figure 10). This suggests absence of intermediate complex formation prior to redox reaction. In addition, the results of the spectroscopic studies indicate no significant shifts from the absorption maxima of

λ_{max} = 630 nm. This further suggests the absence of the formation of an intermediate complex in the reaction.

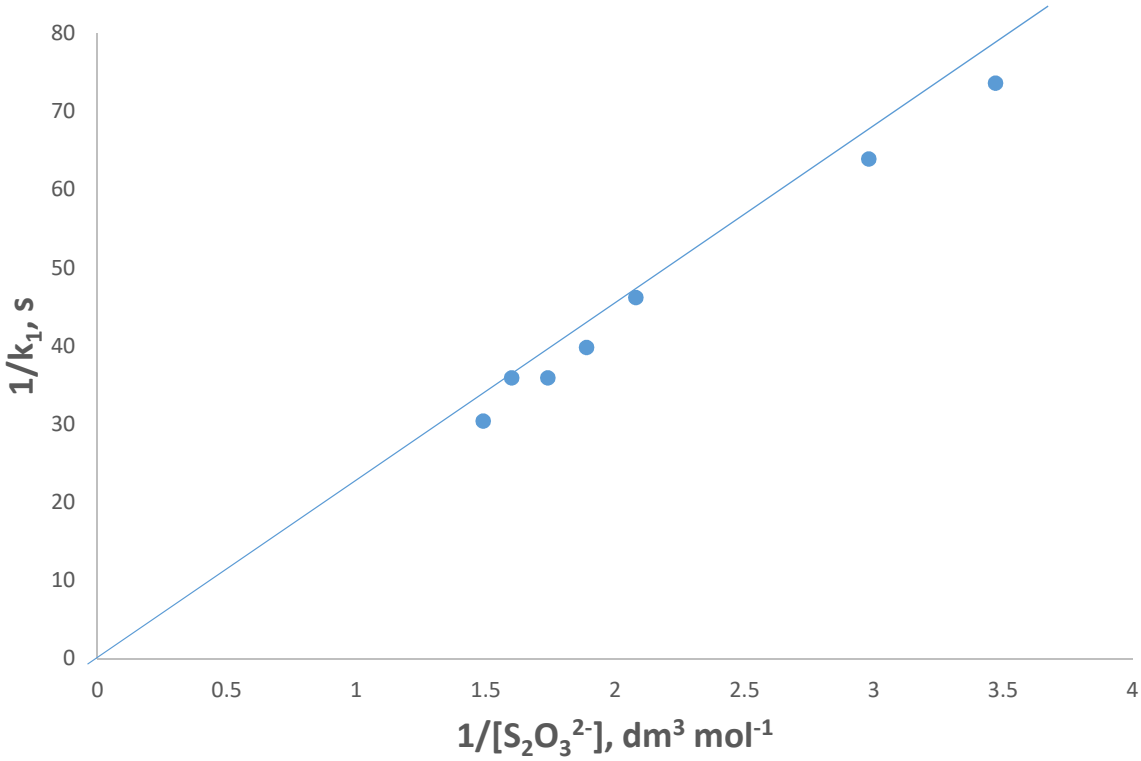

Figure 10: Michaelis-Menten plot of $1/k_1$ versus $1/[S_2O_3^{2-}]$ for the reduction of MG^{2+} by $S_2O_3^{2-}$ at $[MG^{2+}] = 4.8 \times 10^{-5}$ mol dm^{-3}, $[S_2O_3^{2-}] = (0.288 – 0.672)$ mol dm^{-3}, $[H^+] = 1.0 \times 10^{-4}$ mol dm^{-3}, $\mu = 0.06$ mol dm^{-3}(NaCl), T = 29.0 ± 1.0^{O}C and λ_{max} = 630 nm

3.9 Mechanism of the Reaction

The inhibition of the rates of the reaction by the increase in acid concentration as observed in this reaction showed two parallel reaction pathways: the acid independent and the inverse acid dependent pathways. The inverse acid pathway shows that there is a pre- equilibrium step before the rate determining step in which a proton is lost. This means that the two rate controlling steps are preceeded by a rapid equilibrium for which the equilibrium constant is small, and both the forms, protonated and deprotonated, are reactive. Based on the above result, there is a suggestion that the reaction proceeded through two acid dependent and acid independent pathways

$MG^{2+} + S_2O_3^{-2} + H_2O \quad K \quad MG^{+}O^{-} + HS_2O_3^{-} + H^{+}$ 5

$MG^{+}O^{-} + HS_2O_3^{-} \quad k_2 \quad$ Products 6

$MG^{2+} + S_2O_3^{2-} \quad k_3 \quad$ Products 7

Equation 6 and 7 are the rate determining steps, therefore,

$$Rate = k_2[MG^+O^-][HS_2O_3^-] + k_3[MG^{2+}][S_2O_3^{2-}] \quad \ldots\ldots\ldots 8$$

From equation 5

$$[MG^+O^-][HS_2O_3^-] = K[MG^{2+}][S_2O_3^{2-}][H^+]^{-1} \quad \ldots\ldots\ldots 9$$

Substituting equation 9 into 8

$$Rate = k_2[MG^{2+}][S_2O_3^{2-}] + Kk_3[MG^{2+}][S_2O_3^{2-}][H^+]^{-1} \quad \ldots\ldots\ldots 10$$

$$Rate = (a + b\,[H^+]^{-1})\,[MG^{2+}][S_2O_3^{2-}] \quad \ldots\ldots\ldots 11$$

Equation (11) agrees with the experimentally observed rate law (equation 2)

Where $a = k_2 = 4.8 \times 10^{-2}$ dm^3 mol^{-1} s^{-1} and $b = Kk_3 = 1.8 \times 10^{-2}$ dm^6 mol^{-1} s^{-1}

In trying to assign mechanistic pathway for this reaction, the following points are considered:

The Michaelis- Menten plot of $1/k_1$ vs $1/ [S_2O_3^{2-}]$ was linear without an intercept indicating the absence of intermediate complex formation. This suggests the outer-sphere mechanism (Babatunde *et al*., 2013).

Absence of free radicals in the reaction mixture suggests the contribution of outer-sphere mechanism.

Absence of spectrophotometric evidence of intermediate complex formation suggests that a precursor complex is probably not formed prior to electron transfer and that the redox reaction most probably occurs by the outer-sphere mechanism.

3.10 Conclusion

The kinetics of reduction of methyl green by thiosulphate ion under acidic medium was studied, the stoichiometry of the reaction was found to be 1:4 and the reaction was found to follow pseudo-first order kinetics. The rates if the reaction were found to be inhibited by increase in acid concentration, added cations and dielectric constant, whereas increased with increase in ionic strength and added anions. Based on the above kinetic data, the reaction is said to follow outer-sphere mechanism.

References

Babatunde, O.A., Faruruwa, M.D. and Umoru, P.E. (2013). Mechanism of the reduction of 3,7 bis(dimethylamino)phenothionium chloride by metabisulphite ion in acidic medium. Pelagia Reseach Library, 4(3): 69-78.

Barbera, J.J., Metzger, A. and Wolf, M. (2012). Sulphites, Thiosulphates and Dithioites ullmann's Encyclopedia of industrial chemistry, Wiley- VCH, Weinheim, 25, 477.

Cicone, J.S., Petronis, J. B., Embert, C.D. and Spector, D.A. (2004). Successful Treatment of Calciphylaxis with Intravenous Sodium Thiosulphate. *American Journal of kidney disease*. **43** (6): 1104 -1108.

Gibson, C. R. (1908). The Romance of Modern Photography. Its Discovery and its Achievements pp. 37.

Gupta, V.K. and Suhas. (2009). Application of Low-cost Adsorbents for Dye Removal. A Review *Journal of Environmental Management*, **90** (8): 2313 – 2342.

Hall, A. H., Dart. R. and Bogdan, G. (2007). Sodium Thiosulphate or Hydroxocobalamin for the Empiric Treatment of Cyanide Poisoning, **49**: (96), 806 -813.

Mai, F.D., Chem, C.C., Chem, J. C. and Liu, S.C. (2008). Photodegradation of Methyl Green using Visible Irradiation in ZnO Suspentions. *Journal of Chromatograph*, A, **1189** (1-2): 355 – 365.

Mohammed, Y., Iyun, J. F. and Idris, S. O. (2009). Kinetic Approach to the Mechanism of the Redox Reaction of Malachite Green and Permanganate ion in Aqueous Acidic Medium. *African journal of pure and Applied chemistry*. 3(12): 269 – 274.

Osunlaja, A.A. (2013). Kinetics and mechanism of the oxidation of some thioureas by μ-superoxo binuclear Cobalt(III) complexes and 3,7-bis (dimethylamino) phenazothionium chloride in aqueous acidic media. An unpublished Phd Thesis of ABU Zaria.